

## Rotational Symmetry of the $SU(3)$ Potential

A. Hasenfratz<sup>1</sup>, P. Hasenfratz<sup>1</sup>, U. Heller and F. Karsch

CERN, CH-1211 Geneva 23, Switzerland

Received 2 April 1984

**Abstract.** We study the restoration of rotational symmetry of the heavy quark potential obtained from elongated planar and off-axis Wilson loops measured on a  $16^4$  lattice at  $\beta = 5.4$  and  $5.7$ . While the rotational symmetry is still distorted at  $\beta = 5.4$  the potential is consistent with rotational symmetry at  $\beta = 5.7$ . If we were in the asymptotic scaling region the linear slope would correspond at  $\beta = 5.7$  to a string tension  $A_L/\sqrt{\sigma} = 0.0074 \pm 0.0002$ .

### 1. Introduction

Early exploratory studies of  $SU(3)$  lattice gauge theories [1] indicated that continuum physics can be extracted from Monte Carlo simulations performed on rather small lattices at moderate values of the correlation length. These calculations were consistent with asymptotic scaling according to the one-loop  $\beta$  function

$$aA_L = \exp \left\{ -\frac{24\pi^2}{33}g^{-2} + \frac{51}{121} \ln \frac{48\pi^2}{33}g^{-2} \right\} \quad (1)$$

already for  $1/g^2 \gtrsim 0.9$  ( $\beta \equiv 6/g^2 \gtrsim 5.4$ ). However, recent more detailed investigations of the string tension  $\sigma$  [2–4] and critical temperature  $T_c$  [5] on large lattices have shown that the approach to the continuum limit is more subtle than it was previously assumed. Significant deviations from asymptotic scaling have been observed in the regime of coupling constants,  $\beta \simeq 5.4$ – $6$ . The question to what extent we observe continuum physics in present Monte Carlo studies of lattice QCD, even in the pure glue sector, certainly requires further investigations.

One signal for the onset of continuum physics is the restoration of the rotational symmetry of the heavy quark potential [6] which, in the strong coupling regime, is distorted due to the discreteness of the Euclidean space–time lattice. In the case of

$SU(2)$  lattice gauge theory the restoration of the rotational symmetry of the potential has been convincingly demonstrated [6]. For pure  $SU(3)$  gauge theory, the restoration of rotational symmetry has been analyzed in the context of glueball mass spectroscopy in [7] where a restoration of the symmetry for  $\beta \geq 5.5$  has been observed. In this paper we present results for the  $SU(3)$  heavy quark potential at two values of  $\beta$  ( $\beta = 5.4$  and  $5.7$ ) on a  $16^4$  lattice. We analyze the rotational invariance of the potential and determine the string tension from its asymptotic slope. The efficiency of a recently proposed method to suppress statistical fluctuations in the measurement of large Wilson loops [3] (“multi-hit” method) is also investigated. The comparison of conventional and multi-hit measurements at  $\beta = 5.7$  and  $8.0$  shows that the multi-hit method works well for large planar Wilson loops at moderate correlation lengths. This method allows us to determine the potential up to distance  $R = 5a$  at  $\beta = 5.7$ .

### 2. Measurement of Wilson Loops

In order to analyze the heavy quark potential we need the expectation values of Wilson loops

$$W(\hat{C}) = \left\langle \text{Tr} \prod_{i \in \hat{C}} U_i \right\rangle \quad (2)$$

where  $U_i \in SU(3)$  are the usual link variables on the link  $i$  of a four-dimensional hypercubic lattice. The “spatial” parts of the loop  $\hat{C}$  connect the quark–antiquark sources which lie off-axis in general. The “time-like” parts of  $\hat{C}$  are straight lines and the loop is elongated in the time direction (Fig. 1).

The expectation values of Wilson loops have been calculated on configurations generated on a  $16^4$  lattice according to the partition function

$$Z(\beta) = \int \prod_{\substack{\text{links} \\ n,\mu}} dU_{n,\mu} e^{-\beta S(U)} \quad (3)$$

<sup>1</sup> On leave of absence from Central Research Institute for Physics, Budapest, Hungary

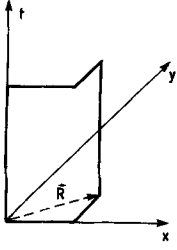


**Fig. 1.** The potential  $V_0(\mathbf{R})$  is determined by measuring spatially elongated Wilson loops. For example, the potential  $V(\mathbf{R} = (2, 1, 0))$  is obtained from the loops of this figure at different, large values of  $T$

where  $S(U)$  denotes the standard Wilson action

$$S(U) = \sum_{\text{plaquettes } n, \mu\nu} (1 - \frac{1}{3} \text{Re Tr } U_{n, \mu} U_{n+\mu, \nu} U_{n+\nu, \mu}^+ U_{n, \nu}^+) \quad (4)$$

We have analyzed 30 configurations at  $\beta = 5.4$  and 40 configurations at  $\beta = 5.7$ . These configurations were taken out of a sample of 50 well-equilibrated configurations separated by 10 full sweeps which have been used previously for spectrum calculations [8]. Our results for the Wilson loop expectation values are summarized in Tables 1 and 2. In order to obtain statistically significant results also for large loops at  $\beta = 5.7$  we have used the “multi-hit” method to measure planar loops with  $R, T \geq 3$ . This method has been used by Parisi et al. [3] to measure Polyakov line correlations at large distances. Also for an  $SU(2)$  gauge group the method leads to a significant reduction in the statistical error of large Wilson loops for couplings in the cross-over region [9]. For the multi-hit measurements, we replace (2) by

$$W(R, T) = \left\langle \text{Tr} \prod_{i \in C} U_i \right\rangle \quad (5)$$

**Table 1.** Measured values of planar and off-axis Wilson loops  $W(R, T)$  at  $\beta = 5.4$  on a  $16^4$  lattice.  $T$  denotes the extent of the loop in the fourth direction. The second column shows the path of length  $R$  in the three spatial directions

R	Path	T						
		1	2	3	4	5	6	7
1	•••	1.4149(26)	0.6939(20)	0.3430(11)	0.1696(10)	0.0843(6)	0.0416(6)	0.0207(5)
1.41	••• •••	0.7836(21)	0.2482(15)	0.0835(10)	0.0288(5)	0.0095(3)	0.0032(3)	0.0007(3)
1.73	••• ••• •••	0.4504(17)	0.1007(10)	0.0258(3)	0.0066(4)	0.0012(4)	0.0007(3)	0.0007(5)
2	••••		0.1810(9)	0.0490(7)	0.0134(3)	0.0041(3)	0.0009(3)	—
2.236	•••• ••••	0.3949(17)	0.0719(10)	0.0144(3)	0.0031(4)	0.0007(3)	0.0006(3)	—
3	•••••			0.0074(3)	0.0010(3)	0.0005(3)	—	—

**Table 2.** Same as Table 1 but at  $\beta = 5.7$ . The star indicates loops measured with the multi-hit method of [3]

R	Path	T						
		1	2	3	4	5	6	7
1	•••	1.6470(30)	0.9734(18)	0.5848(12)	0.3528(7)	0.2127(6)	0.1284(5)	0.7743(4)
1.41	••• •••	1.0804(19)	0.5018(12)	0.2487(6)	0.1253(4)	0.0630(3)	0.0323(5)	0.0163(3)
1.73	••• ••• •••	0.7360(17)	0.2890(9)	0.1277(7)	0.0586(4)	0.0272(5)	0.0123(4)	0.0051(5)
2	••••		0.3962(14)	0.1725(10)	0.0763(6)	0.0343(3)	0.0152(3)	0.0067(3)
2.236	•••• ••••	0.6609(17)	0.2293(11)	0.0915(5)	0.0379(4)	0.0158(3)	0.0064(3)	0.0030(3)
2.45	•••• ••••	0.4555(11)	0.1380(3)	0.0510(4)	0.0195(4)	0.0812(2)	0.0313(4)	0.0139(3)
2.83	•••• ••••	0.4226(101)	0.1158(48)	0.3953(18)	0.0140(9)	0.0051(4)	0.0022(3)	0.0088(4)
3	•••••*			0.05824(38)	0.02078(25)	0.00746(13)	0.00273(7)	0.00098(4)
3.16	••••• •••••	0.3998(10)	0.1026(9)	0.0327(3)	0.0114(3)	0.0036(4)	0.0012(3)	0.0004(3)
4	••••••*				0.00609(17)	0.00182(8)	0.00055(3)	0.00016(3)
5	•••••••*					0.00049(3)	0.00012(2)	0.00003(1)

where  $\bar{U}_i \equiv U_i$  for the first and last link on the two time-like sides of the Wilson loop and

$$\bar{U}_i = \int dU_i \exp \left\{ \frac{\beta}{6} \text{Tr} U_i X_i^+ + \text{h.c.} \right\} \cdot U_i / \int dV_i \exp \left\{ \frac{\beta}{6} \text{Tr} V_i X_i^+ + \text{h.c.} \right\} \quad (6)$$

elsewhere. Here  $X_i^+$  denotes the sum of the six ordered products of the three remaining links completing the plaquettes which contain the link variable  $U_i$ . Contrary to the case of  $SU(2)$ , where the integral, (6), can be done analytically [9], one has to evaluate  $\bar{U}_i$  numerically in the case of  $SU(3)$ . We have analyzed 15 configurations at  $\beta = 5.7$  using the above multi-hit method. The one-link integral, (6), has been evaluated using the Cabibbo–Marinari heat bath algorithm [10] with three  $SU(2)$  subgroup updates and 15 hits for each of them. The results of these measurements are included in Table 2. To check the advantage of this method over conventional loop measurements we compare in Table 3 the results obtained in both ways for large loops. The time requirement for the analysis of a given configuration using the multi-hit method (with 15 hits) was about a factor 10 larger than for a conventional measurement. However, taking into account the creation time for one new independent configuration, this reduces to a factor  $\sim 3$ –4. One may thus conclude that the multi-hit method is preferable, whenever the statistical error obtained on a given set of configurations is smaller by a factor of  $\sim 2$ . At  $\beta = 5.7$  this is certainly the case for planar loops with  $R + T \gtrsim 8$ . We performed a similar comparison at  $\beta = 8$  where it was found that the multi-hit method did not reduce the statistical error significantly. This is understandable as at  $\beta = 8$  the correlation length is already so large that the averaging procedure involved in the multi-hit method, (6), is not necessary to smooth the distribution of link variables.

**Table 3.** Comparison of large Wilson loops  $W(R, T)$  measured with the conventional method (a) on 40 configurations at  $\beta = 5.7$  and using the multi-hit method of [3], (b) on 15 configurations

$R$	$T$	$W(R, T)(a)$	$W(R, T)(b)$
3	4	0.02109(31)	0.02078(25)
	5	0.00746(35)	0.00746(13)
	6	0.00273(24)	0.00273(7)
	7	0.00076(31)	0.00098(4)
4	4	0.00616(26)	0.00609(17)
	5	0.00178(33)	0.00182(8)
	6	0.00059(38)	0.00055(3) 0.00016(3)
5	5		0.00049(3)
	6		0.00012(2)
	7		0.00003(1)

### 3. The Heavy Quark Potential

The ground state energy of a pair of heavy quarks and antiquarks separated by a distance  $\mathbf{R}$  can be expressed in terms of the expectation values of the Wilson loops of Fig. 1 as

$$V_0(\mathbf{R}) = \lim_{T \rightarrow \infty} \ln [W(\mathbf{R}, T-1)/W(\mathbf{R}, T)]. \quad (7)$$

$V_0(\mathbf{R})$  is the dimensionless lattice potential which still contains an additive (divergent, non-physical) self-energy contribution. This additive constant should be removed when the scaling properties of the potential are investigated [11]. The slope of the linear part of the potential is, of course, not influenced by this constant.

In practice, the limit  $T \rightarrow \infty$  cannot be taken and only finite  $T$  approximants to (7) can be calculated on finite lattices. For finite  $T$  the Wilson loop expectation values are built up by a superposition of excited states in addition to the ground state contribution  $V_0(\mathbf{R})$

$$W(\mathbf{R}, T) = c_0 e^{-V_0(\mathbf{R})T} + c_1 e^{-V_1(\mathbf{R})T} + \dots \quad (8)$$

with non-negative coefficients  $c_\alpha$ . This ensures that for any  $T$  the approximants

$$V_T(\mathbf{R}) = \ln [W(\mathbf{R}, T-1)/W(\mathbf{R}, T)] \quad (9)$$

are an upper bound for the potential  $V_0$  at distance  $\mathbf{R}$ . In fact, in practice,  $V_T(\mathbf{R})$  describes the asymptotic behaviour well as soon as  $T \gtrsim |\mathbf{R}| + 1$  [12]. This can be seen in Fig. 2, where the approximants  $V_T(\mathbf{R})$  are plotted as a function of  $T$  for different values of  $\mathbf{R}$ .

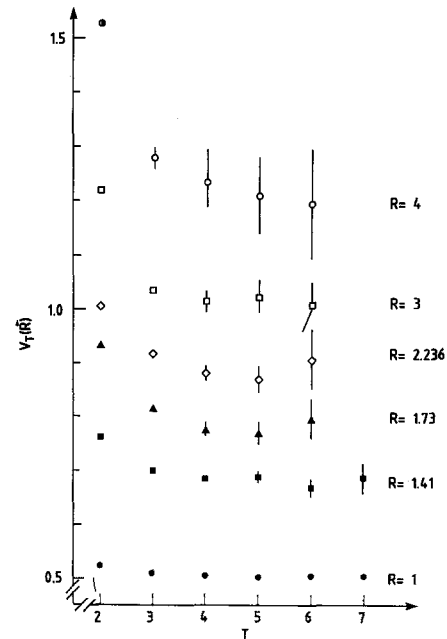


**Fig. 2.** Logarithms of Wilson-loop ratios  $V_T(\mathbf{R}) = \ln [W(\mathbf{R}, T-1)/W(\mathbf{R}, T)]$ . The Wilson loops have been measured on a  $16^4$  lattice at  $\beta = 5.7$

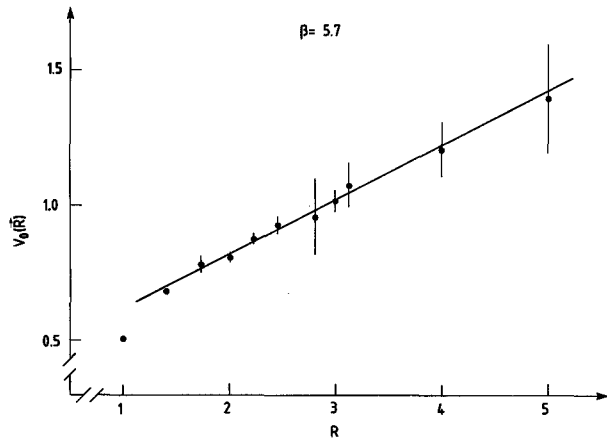


**Fig. 3.** The heavy quark potential  $V_0(\mathbf{R})$  versus  $R \equiv |\mathbf{R}|$  measured on a  $16^4$  lattice at  $\beta = 5.7$ .  $V_0(\mathbf{R})$  is determined from the average of the approximants  $V_T(\mathbf{R})$ ,  $T = 4, 5, 6$  for  $R \leq 3.16$ ;  $T = 5, 6, 7$  for  $R = 4$  and  $V_0(\mathbf{R}) = V_T(\mathbf{R})$ ,  $T = 6$  for  $R = 5$ . The solid line is a least square fit to the data:  $V_0(\mathbf{R}) = 0.42 + 0.20R$

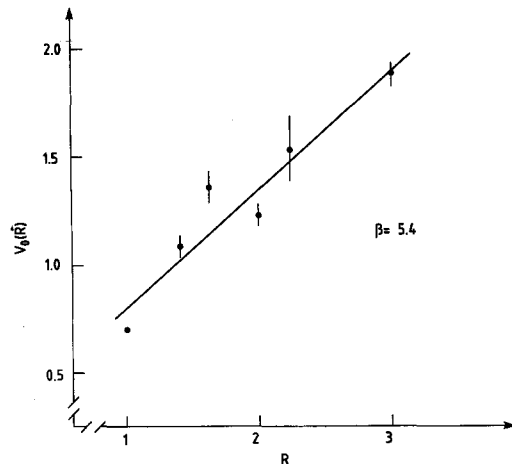


**Fig. 4.** Same as Fig. 3 but at  $\beta = 5.4$ .  $V_0(\mathbf{R})$  is determined from the average of the approximants  $V_T(\mathbf{R})$ ,  $T = 4, 5, 6$  for  $R \leq 1.5$ ;  $T = 4, 5$  for  $R = 2$  and  $V_0(\mathbf{R}) = V_T(\mathbf{R})$ ,  $T = 4$  for  $R = 1.73, 2.236$  and 3. The solid line is a least square fit to the data:  $V_0(\mathbf{R}) = 0.24 + 0.56R$

If rotational symmetry is restored,  $V_0(\mathbf{R}) = V_0(|\mathbf{R}|)$ , and  $V_0(\mathbf{R})$  plotted against  $|\mathbf{R}|$  is a smooth, single valued function of  $|\mathbf{R}|$ . This is really the case at  $\beta = 5.7$  (Fig. 3). Within the statistical errors, the points are consistent with rotational symmetry at this coupling. Additionally, there is an early onset of linear behaviour: for  $|\mathbf{R}| \geq 1.5$  the potential is well described by the form

$$V_0(\mathbf{R}) = a + b|\mathbf{R}|, \quad |\mathbf{R}| \geq 1.5, \quad \beta = 5.7. \quad (10a)$$

A least square fit gives

$$a = 0.43 \pm 0.01; \quad b = 0.195 \pm 0.01. \quad (10b)$$

From the slope  $b$  of the potential we can determine the string tension  $\sigma$  in units of  $A_L$ . Using (1) this yields

$$A_L/\sqrt{\sigma}(\beta = 5.7) = 0.0074 \pm 0.0002 \quad (11)$$

in accordance with earlier determinations of  $A_L/\sqrt{\sigma}$  at this value of  $\beta$  [2]. Clearly, the situation is different at  $\beta = 5.4$  (Fig. 4). Here the rotational symmetry of the potential is still distorted due to lattice artifacts. The points are not consistent with a smooth curve. A linear fit to the potential gives  $V_0(\mathbf{R}) = 0.24 + 0.56|\mathbf{R}|$ , but the points scatter widely around this curve.

#### 4. Conclusions

We have analyzed the rotational invariance properties of the SU(3) heavy quark potential. While the rotational symmetry is still distorted at  $\beta = 5.4$  we find a rotationally invariant potential at  $\beta = 5.7$ . This observation raises the possibility that for  $\beta \geq 5.7$  continuum behaviour might already be present. In this case the physical quantities should scale, although not necessarily according to the asymptotic form of (1), but governed by the full  $\beta$ -function.

*Acknowledgements.* We thank R. Petronzio for discussions and help in the early stages of this work.

#### References

1. M. Creutz: Phys. Rev. **D21**, 2308 (1980); E. Pietarinen: Nucl. Phys. **B190**, [FS3], 349 (1981)
2. F. Gutbrod, P. Hasenfratz, Z. Kunzst, I. Montvay: Phys. Lett. **128B**, 415 (1983)
3. G. Parisi, R. Petronzio, F. Rapuano: Phys. Lett. **128B**, 418 (1983)
4. J.D. Stack: ITP-Santa Barbara Preprint N° 136 (1983)
5. F. Karsch, R. Petronzio: Phys. Lett. **139B**, 403 (1984); Ph. de Forcrand, C. Roiesnel: Ecole Polytechnique Preprint (1983)
6. C.B. Lang, C. Rebbi: Phys. Lett. **115B**, 137 (1982)
7. G. Schierholz, M. Teper: Phys. Lett. **136B**, 64 (1984)
8. P. Hasenfratz, I. Montvay: DESY Preprint DESY 83-072 (1983)
9. F. Karsch, C.B. Lang: Phys. Lett. **138B**, 176 (1984)
10. N. Cabibbo, E. Marinari: Phys. Lett. **119B**, 387 (1982)
11. J.D. Stack: Phys. Rev. **D27**, 412 (1983); F. Gutbrod, I. Montvay: Scaling of the Quark-Antiquark Potential and Improved Actions in SU(2) Lattice Gauge Theory DESY Preprint DESY 83-112 (1983)
12. A similar observation has been made for the U(1) lattice gauge theory in: J. Jersak, T. Neuhaus, P.M. Zerwas: Aachen Preprint PITHA 83/16 (1983)